Mapping stress in polycrystals with sub-10 nm spatial resolution

Supplementary material

C. Polop,[a*] E. Vasco,[b] A. P. Perrino[b] and R. Garcia[b]

[a] *Departamento de Física de la Materia Condensada and Instituto Nicolás Cabrera, Universidad Autónoma de Madrid, 28049 Madrid, Spain.* [b] *Instituto de Ciencia de Materiales de Madrid, CSIC, Sor Juana Inés de la Cruz 3, 28049 Madrid, Spain*

1) Characterization by scanning electron microscopy and x-ray diffraction

The microstructure and crystallinity of the samples were investigated by scanning electron microscopy (SEM) and x-ray diffractions (XRD). The SEM images were acquired in a Philips XL-30 FEG microscope operating at 5 kV; while the XRD measurements were taken in an X'Pert four-circle diffractometer using Cu K_α radiation. Fig. 1s shows the results obtained from both characterizations for 600 nm and 1200 nm-thick Au films on mica substrates. The films exhibit a columnar structure (Figs. 1s-a and 1s-b) with an out-of-plane [111] texture (Fig. 1s-c) and without in-plane order as measured by Phi-scan XRD (not shown here).

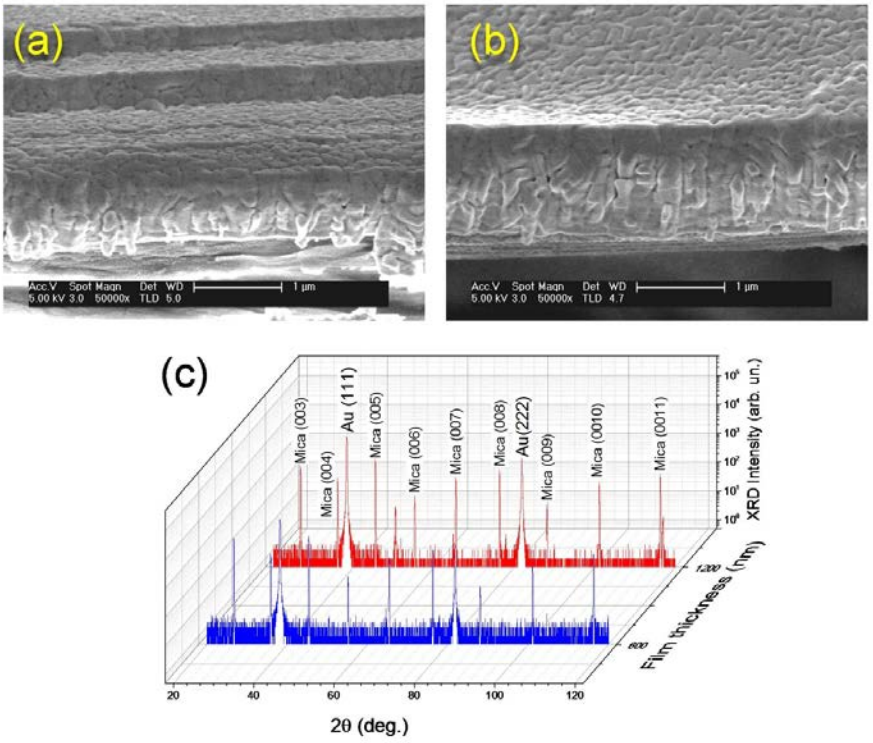

Fig. 1s Ex-situ sample characterization. (a, b) Cross-section SEM images of 600 nm and 1200 nm-thick Au films on mica substrates, respectively. (c) θ-2θ XRD scans of the same films.

2) Intrinsic stress evolution during film deposition

For the in-situ stress characterization, Au films were deposited at the same grown conditions reported in the manuscript with the exception of the substrate. In this case, Si(100) substrates were used to get the mirror reflectivity required for the multibeam optical stress sensor (MOSS). The substrates were cut in form of bin (with typical sizes of 15x3 mm), and fixed to the sample holder at one end, such that the greater part of its volume remains suspended to avoid mechanical constrictions of the sample curvature. The obtained films are formed by a compact array of [111]-textured columns with microstructure and morphology analogous to those Au films deposited on mica.

The in-situ real-time characterizations were carried out by means of a MOSS similar to that proposed by Floro and Chason [1,2]. The collimated beam of a λ=532 nm-Si photodiode laser (with power of 10 mW) is decomposed into multiple parallel beams by a single Silica etalon. The parallel beams are mirror reflected on the sample surface at 45^{o}, filtered by a 532 nm-centered bandpass filter (which removes the background, particularly the IR radiation emitted by the evaporator) and collected at 30 fps in a high-resolution CCD camera (by Hamamatsu) with a CCD element size of 6 μm. The step-up was implemented on anti-vibration platform to minimize high frequency (>10 Hz) noise, and a laser-position stabilization system was included to prevent the spherical aberrations caused by collective beam displacements (i.e., the sensor is sensitive only to relative displacements). This sensor allows us to investigate simultaneously the evolutions of: (a) the sample curvature up to 1/40 km^{-1} from the relative displacements of the beams (with an uncertainty of ±0.05 pixels), and (b) the mirror reflectivity of the sample from the beam intensities. By applying the Stoney equation [3], we can relate the average stress in the film to the sample curvature; while through the Fresnel equations modified to account for the light reflection/transmission at rough interfaces between non-opaque media [4,5], we can estimate the deposition rate, the thickness of the layer of native oxide on Si as well as the time-scaling of the surface roughness.

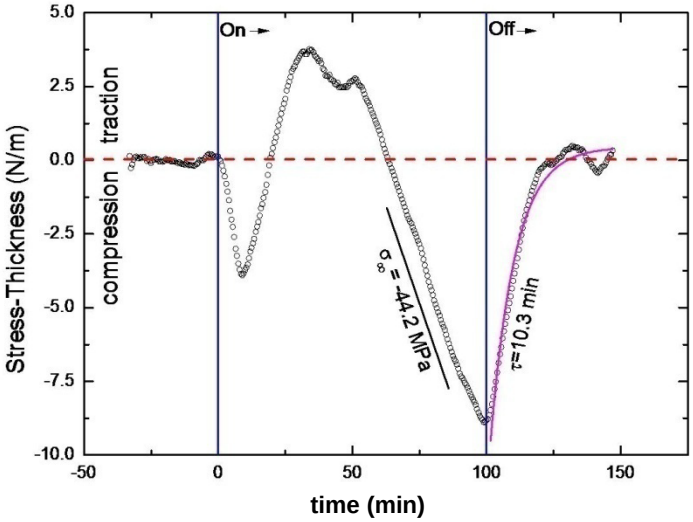

Fig. 2s. Stress-thickness evolution of an Au film deposited on (100)Si at a rate of F =0.1 nm/s. Vertical lines denotes the flux-on and flux-off transients. The solid curve corresponds to the fitting dependences (namely, stress-thickness $\propto F\sigma_{\infty}t$ for a constant flux or $\propto \exp(\pm t/\tau)$ for flux transients) together their parameters.

Figure 2s shows the stress-thickness evolution as a function of the deposition time for Au films. The stress-thickness curve exhibits the typical compression-traction-compression behavior that characterizes to the polycrystalline film growing by Volmer-Weber mode under high mobility conditions. From the curve, we get a steady postcoalescence compression of -44.2 MPa, which relaxes at a rate of $1/\tau \approx$ 1.6 mHz once the flow is stopped, such that the compressive stress at macroscopic scale has been mostly released after 1 h. This time is shorter than that used to remove the sample from the deposition system and place it in our scanning probe microscopy set-up.

3) Details of the simulation of stress-stiffening effect by Finite Element Modeling

Figure 3s shows relevant details of the involved geometry as well as intermediate results of the simulating of the stress-stiffening effect by Finite Element Modeling (FEM). This information complements that provided by Ref. [29] in the main text.

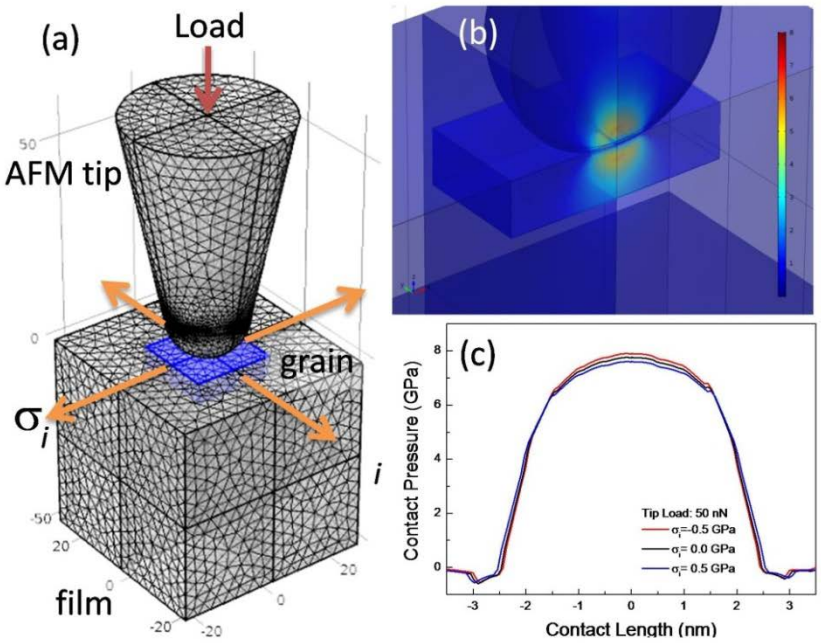

Fig. 3s. Stress-stiffening simulation by FEM. (a) Involved geometry consisting of a biaxially pre-stressed grain (embedded within the volume of a film, slab) on which a conical tip with spherical apex exerted a load. Although the displayed mesh structure corresponds to that used for the simulation, its density was reduced for the sake of the visualization. (b) 3D distribution of the contact pressure for a tip load of 50 nN on a grain with a pre-compression of -0.5 GPa. (c) 2D profiles of the contact pressure along the grain diameter for different pre-stresses (see legend).

References

1 J. A. Floro and E. Chason, *Appl. Phys. Lett.*, 1996, **69**, 3830

2 J. A. Floro, E. Chason, S. R. Lee, R. D. Twesten, R. Q. Hwang and L. B. Freund, *J. Electronic Mater.*, 1997, **26**, 969

3 G. G. Stoney, *Proc. Roy. Soc.*, 1909, **A82**, 172

4 H. E. Bennett and J. O. Porteus, *J. Opt. Soc. Am.*, 1960, **51**, 123

5 G. Le´rondel and R. Romestain, *Appl. Phys. Lett.*, 1999, **74**, 2740